

Synthesis and characterization of selenium nanoparticles stabilized by pumpkin polysaccharide

Quan Thi Thu Trang, Nguyen Binh Duong, Phan Thi Ngoc Bich*

Institute of Chemistry, Vietnam Academy of Science and Technology, 18 Hoang Quoc Viet, Nghia Do, Hanoi, Vietnam.

*Corresponding author: bich@ich.vast.vn

Received 8 Sep. 2025; Revised 10 Nov. 2025; Accepted 10 Dec. 2025; Published 25 Dec. 2025.

DOI: <https://doi.org/10.54939/1859-1043.j.mst.108.2025.83-90>

ABSTRACT

This study presents a green synthesis of selenium nanoparticles from Na_2SeO_3 using ascorbic acid as the reducing agent in the presence of pumpkin polysaccharide (PP). PP was employed as a stabilizing and dispersing agent for selenium nanoparticles (SeNPs), which has not been reported in previous studies. The obtained material was characterized using UV-Vis spectrophotometry, XRD, FTIR, SEM, TEM, EDX, and zeta potential analyses. FTIR profiles revealed that PP capped the SeNPs surface through hydrogen bonding and electrostatic interactions involving hydroxyl and carboxylate groups. Microscopic observations further showed that PP markedly improved the particle morphology of PP-SeNPs, producing nanoparticles with enhanced dispersion, reduced aggregation and a dominant size range of 65 - 100 nm, compared with 75 - 160 nm for uncapped SeNPs. The enhanced colloidal stability was supported by a significantly more negative zeta potential (-22.9 mV versus -8.7 mV for pure SeNPs). Acute toxicity testing demonstrated that PP-SeNPs exhibited low toxicity, with an LD_{50} value of 945.83 mg/kg. These results suggest that PP offers a promising platform for SeNPs and may support their future biomedical applications.

Keywords: Selenium nanoparticles; Pumpkin; Polysaccharide; Stability; Acute toxicity.

1. INTRODUCTION

Today, selenium is well recognized as an essential trace element for human health. In the body, selenium primarily exists in the form of selenocysteine within selenoproteins, which are responsible for a wide range of vital physiological functions. Consequently, selenium deficiency can lead to serious health problems, including impaired antioxidant defense systems, weakened cardiovascular and immune function, thyroid hormone metabolism disorders, neurological dysfunction, and other disease conditions. Selenium adequate supplementation has been shown to help prevent some cancers (bowel, lung, and prostate cancer) and reduce the risk of cardiovascular diseases, autoimmune thyroid disease and inflammatory disorders. Recently, growing interest has been directed toward the use of selenium in disease prevention and treatment, as well as its potential as a therapeutic agent [1-3].

However, selenium excess (selenosis) also causes adverse effects in humans, ranging from mild symptoms such as weight loss and hair loss to severe consequences, including death, depending on the degree of exposure. Moreover, the therapeutic window of selenium is narrow, which significantly limits its biomedical applications. Therefore, reducing toxicity while improving therapeutic efficacy is a critical challenge for the biomedical use of selenium in general [4, 5].

In recent years, selenium nanoparticles (SeNPs) have attracted considerable attention due to their high bioavailability and, particularly, their lower toxicity compared to both inorganic and organic selenium compounds. Numerous animal studies indicate that SeNPs show comparable or even higher biological activity than organic selenium, while demonstrating significantly reduced toxicity in terms of acute and subchronic toxicity, acute liver damage, and survival rates. Compared to inorganic selenium salts, SeNPs have been found to possess 7-10 times lower

toxicity. As a result, SeNPs have emerged as a promising selenium source for biomedical developments [6, 7]. Many templates, including proteins, polyphenols, polysaccharides, and amino acids, have been used as stabilizers and dispersing agents in order to prepare stable and uniform SeNPs [6, 8]. Among them, the synthesis of SeNPs using polysaccharides has gained significant interest. As an abundant source of natural biopolymers, polysaccharides are generally considered non-toxic, biocompatible and biodegradable, highly suitable for biomedical material development [9, 10]. Chen et al. demonstrated that chitosan (CS) and carboxymethyl-chitosan (CCS) can stabilize selenium nanoparticles, yielding monodispersible SeNPs with an average size of about 50 nm [11]. Qiu et al. reported the fabrication of selenium nanoparticles decorated by pectin from citrus peels and confirmed that pectin as a surface decorator could be effectively used to improve the stability and antioxidant capacity of SeNPs remarkably [12]. More recently, Wang et al. [13] reported that SeNPs coated with sweet corn polysaccharides (SCP-SeNPs) demonstrated promising hypoglycemic, hypolipidemic, and antioxidant properties in type 2 diabetes (T2DM) mice, effectively alleviating diabetes-induced damage in their liver, colon, and kidney tissues.

In this study, we aimed to synthesize SeNPs in the presence of a polysaccharide extracted from pumpkin (PP) to investigate the role of PP in the formation of selenium nanoparticles and examine their acute toxicity. Pumpkin is widely available and abundant, and its polysaccharides can be obtained through a green, straightforward extraction procedure with high efficiency, providing practical advantages for large-scale preparation. More importantly, PP possesses distinctive structural features - such as branched pectic polysaccharides rich in galactose, glucose, arabinose, and uronic acids - that contribute to its favorable biocompatibility and biodegradability. Previous studies have also highlighted several functional bioactivities of PP, particularly their antioxidant, anti-inflammatory, hypoglycemic, and hypolipidemic effects [14, 15]. These attributes make PP a promising natural matrix for stabilizing and functionalizing SeNPs in biomedical and nutraceutical applications. However, the use of PP in the biosynthesis of selenium nanoparticles has not been described in previous studies.

2. EXPERIMENTAL

2.1. Materials

Fresh pumpkin (*Cucurbita moschata*) was purchased from a local market in Hanoi, Vietnam. Sodium selenite (Na_2SeO_3) and other analytical-grade chemicals (ascorbic acid, ethanol, n-hexane, oxalic acid) were of analytical grade, purchased from Xilong Scientific Co., Ltd. (China).

2.2. Preparation of polysaccharide

Polysaccharide was extracted from pumpkin pulp using hot water extraction [16]. Briefly, a mixture of fresh pumpkin pulp and distilled water (ratio of 1:2 w/w) was heated at 80 °C for 4 hours. The mixture was then evaporated to approximately half of its volume and defatted with n-hexane (volume ratio of solution: n-hexane = 3:1). Finally, the mixture was added with 4 times the volume of absolute ethanol, kept overnight at 4 °C and centrifuged to collect the precipitate, which was then freeze-dried to obtain PP. The extraction process produced a relatively high PP yield of about 0.72% calculated on the weight of fresh pumpkin, which is consistent with previously reported values for PP obtained under green and mild extraction conditions [16].

The weight-averaged molecular weight (MW) of PP was analyzed by gel permeation chromatography (GPC) on an Agilent 1100 HPLC system with a refractive index detector, ultrahydrogen 2000 A column and pullulan standard. The sample concentration was 1mg/mL, the eluent was a mixture of 5 mM Na_2CO_3 and 10 mM NaHCO_3 with a flow rate of 1.0 mL/min. The Mw value of PP was found to be 110.59 kDa. PP was also identified using infrared spectroscopy (FTIR, performed as in subsection 2.4).

2.3. Synthesis of PP-SeNPs

A chemical reduction method with ascorbic acid as a reducing agent in the presence of PP as a

capping and stabilizing agent was used to prepare PP-SeNPs. The synthesis was performed according to a previously reported method with several modifications [17], as described below. A volume of 100 ml of 0.03 M Na₂SeO₃ solution was added to a round-bottom flask containing 100 ml of PP solution (2.0 mg/mL) under stirring. Next, 100 ml of 0.09 M ascorbic acid solution was slowly dropped into the flask. The final concentrations of PP, Na₂SeO₃ and ascorbic acid were 2.0 mg/mL, 0.02 M and 0.06 M, respectively, corresponding to a molar ratio of Na₂SeO₃:ascorbic = 1:3. During the dropwise addition, 0.02 M citric acid solution was simultaneously introduced to adjust the pH of the reaction medium to 6.5 - 7.0. The reaction was maintained for 4 h after the completion of ascorbic acid and then left to stand for the next 24 h. The resulting precipitate was collected by centrifugation at 8000 rpm, washed several times with distilled water, and freeze-dried for approximately 24 h to obtain PP-SeNPs. All syntheses were performed at room temperature (approximately 25 °C).

A pure SeNPs sample (without PP) was prepared following the same procedure.

2.4. Characterization of PP-SeNPs

The UV-Vis spectra were recorded on a Hach Dr6000 UV-Vis spectrophotometer with water as the reference over the range of 200 - 700 nm. X-ray diffraction (XRD) patterns were obtained in the range of $2\theta = 10^\circ - 70^\circ$ with a scan rate of 0.03°/s using a D8 Advance (Bruker). FTIR spectra were recorded using an Affinity-S1 spectrophotometer (Shimadzu). Morphology was examined using field emission scanning electron microscopy (FESEM, S4800-Hitachi; sample coated with a thin layer of platinum) and transmission electron microscopy (TEM, JEOL JEM-1010; sample sonicated in distilled water for 30 min and deposited onto carbon-coated copper grids). Selenium content was determined using energy-dispersive X-ray spectroscopy (EDX) on the same FESEM instrument. Zeta potential measurements were obtained by dynamic light scattering (DLS) using a Litesizer 500 (Anton Paar).

2.5. Acute toxicity test

Animals:

White ICR mice (19-22 g) were maintained under standard conditions of temperature and light.

Experimental design:

Mice were randomly divided into 8 groups (6 mice per group) and fasted for 16 h prior to testing. PP-SeNPs were dispersed in distilled water and sonicated for 30 min before being oral administered. Group 1 (control): 0.3 mL of distilled water. Groups 2-8: PP-SeNPs administered at 200, 500, 700, 850, 1000, 1150 and 1300 mg/kg BW, respectively.

Mice were observed for behavioral changes during the first 2 h after administration and monitored for 3 days thereafter.

The acute toxicity value (LD₅₀) was calculated using the Karber-Behrens formula [18]:

$$LD_{50} = LD_{100} - \Sigma a \times b / N$$

Where: LD₅₀ - Dose causing 50% mortality; LD₁₀₀ - Dose causing 100% mortality; N - Number of animals per group; a - Dose difference between two consecutive groups; b - Average mortality between two consecutive groups.

Data were expressed as mean ± SD. Statistical significance was analyzed using Student's t-test, with P < 0.05 considered significant.

3. RESULTS AND DISCUSSION

3.1. Characterizations of PP-SeNPs

During the addition of ascorbic acid to the Na₂SeO₃ solution in the presence of PP, the initially colorless mixture gradually turned orange, and the final product became brownish-red. This progressive color change during the reaction is a visual indication of SeNPs formation.

It is well known that selenium nanoparticles exhibit a characteristic UV-Vis absorption band, typically located in the range of 260 - 350 nm, which is attributed to the localized surface plasmon resonance (LSPR) of nanoscale selenium [19]. The UV-Vis spectra of PP-SeNPs, SeNPs, Na₂SeO₃, and PP are shown in figure 1a. Na₂SeO₃ displayed a single absorption peak at 212 nm, consistent with previous reports [17], while PP showed no detectable absorption in the examined spectral region, in agreement with studies indicating that the polysaccharide had been effectively purified from nucleic acids and proteins [20]. Therefore, the maximum absorption peaks observed at approximately 270 nm for PP-SeNPs and 266 nm for SeNPs can be attributed to the LSPR of selenium nanoparticles. These spectral features confirm that Na₂SeO₃ was fully reduced to elemental selenium in both reaction systems.

Although the markedly smaller particle size of PP-SeNPs (described below) would normally be expected to induce a blue shift of the LSPR peak, the PP-SeNPs spectrum instead showed a slight red shift compared with SeNPs. This suggests that PP modified the surface electron density and local dielectric environment of the nanoparticles, thereby reversing the shift direction of the LSPR peak.

XRD analysis was performed to elucidate the crystalline characteristics of the obtained PP-SeNPs. Both PP-SeNPs and SeNPs (figure 1b) exhibited broad diffraction halos at $2\theta = 20\text{-}30^\circ$ and $45\text{-}55^\circ$, which are typical of amorphous selenium nanoparticles [13]. The stronger peak broadening in the $20\text{-}30^\circ$ region and the near-disappearance of the $45\text{-}55^\circ$ halo in the PP-SeNPs pattern indicate that their particle size was substantially smaller than that of the uncapped SeNPs.

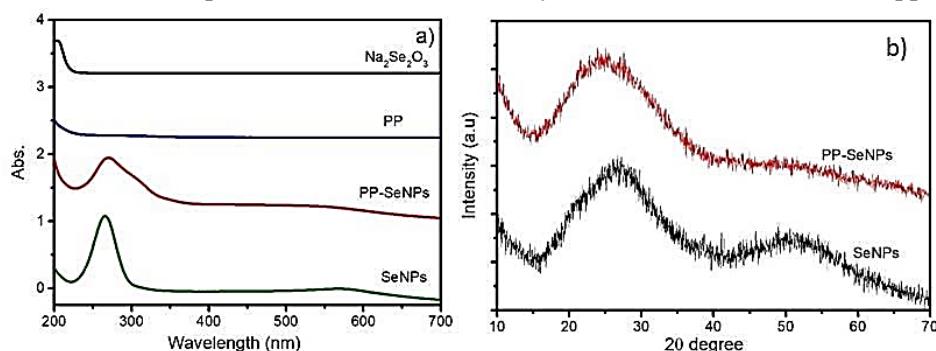


Figure 1. (a) UV-Vis spectra of Na₂SeO₃, PP, SeNPs and PP-SeNPs; (b) XRD patterns of SeNPs and PP-SeNPs.

FTIR spectra were recorded to identify the interactions between functional groups of PP and the SeNPs surface. The results are shown in figure 2. In the spectrum of PP, the broad, strong absorption band observed at 3406 cm^{-1} is attributed to the O-H stretching vibration, indicating the presence of a large number of OH groups in the pyranose ring. The band at 2936 cm^{-1} is assigned to the C-H stretching vibration of CH₂ groups, the small band at around 1746 cm^{-1} , corresponds to the stretching vibration of the C=O. The bands at 1617 and 1415 cm^{-1} are due to COO⁻ asymmetric and symmetric stretching vibration of carboxyl groups, respectively. The weak band at 1266 cm^{-1} is assigned to the side-chain vibrations. The region from $1140\text{-}1040\text{ cm}^{-1}$ is characteristic of the pyranose ring of pectin (C-O and C-OH stretching from glycosidic linkages). And the band at 925 cm^{-1} is typical for vibrations of the C-O-C bridge in polysaccharides [21, 22].

The FTIR spectrum of PP-SeNPs is similar to that of PP, indicating the formation of SeNPs in the PP network. However, several significant changes were observed compared with PP alone. The shift of the OH stretching band (from 3406 to 3421 cm^{-1}), and the COO⁻ stretching band (from 1618 to 1634 cm^{-1}), demonstrate the occurrence of hydrogen bonding and electrostatic interactions of OH⁻ and COO⁻ groups of PP with SeNPs, respectively. Furthermore, a distinct absorption band appeared at 1525 cm^{-1} which could be related to the formation of weak surface complexes between

the carboxyl groups of pectin and the surface of SeNPs [23]. These observations clearly demonstrate the participation of PP in the reaction process, playing a crucial role in SeNPs formation. The SeNPs surface was capped by PP through hydrogen bonding of hydroxyl groups and electrostatic interactions or weak surface complexes of carboxylate groups on the PP chain.

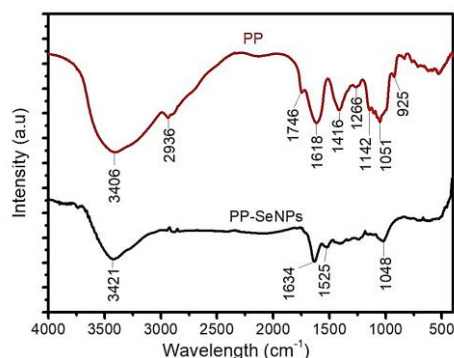


Figure 2. FTIR spectra of SeNPs and PP-SeNPs.

SEM and TEM images were used to analyze the morphology and particle size of selenium nanoparticles (figure 3). In figures 3a and 3b, the SEM and TEM images of PP-SeNPs show nearly spherical nanoparticles with improved dispersion and reduced aggregation. ImageJ analysis showed predominant particle sizes in the range of 65 - 100 nm with an average size of 80.8 ± 12.46 nm. In contrast, in the pure SeNPs sample without PP (figure 3c and 3d), the selenium nanoparticles are significantly larger and more irregular, with the estimated particle sizes of 75 - 160 nm and more importantly, they are evidently aggregated. These results highlight the ability of PP to control size and effectively prevent the aggregation of SeNPs.

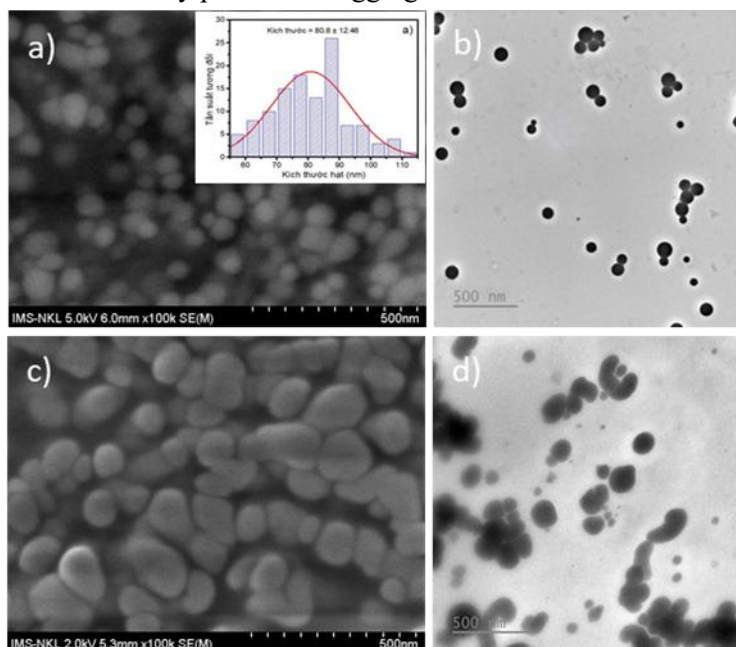


Figure 3. (a) SEM; (b) TEM images of PP-SeNPs; (c) SEM; (d) TEM images of SeNPs.

The EDX spectrum (figure 4) displayed a strong characteristic selenium peak at about 1.5 keV, along with weak peaks corresponding to C and O elements. This implies the existence of selenium within an organic matrix of PP. The Se content in PP-SeNPs was determined to be 47.27%.

The nanoparticle stability is an important parameter for practical applications. The zeta

potential, which indicates the electrostatic repulsion between particles, is a good indicator for predicting long-term storage stability of SeNPs in dispersion. The closer this value is to zero, the more easily the nanoparticles tend to aggregate. As shown in figure 5, PP-SeNPs exhibited a zeta potential of -22.9 mV, significantly higher in magnitude than that of pure SeNPs (-8.7 mV), indicating enhanced colloidal stability provided by the PP capping layer. The zeta potential value of PP-SeNPs aligns with previous studies on polysaccharide-mediated SeNPs [13, 24].

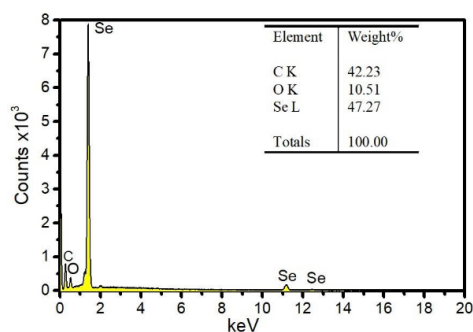


Figure 4. EDX spectrum of PP-SeNPs.

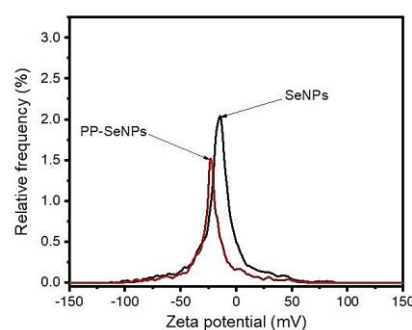


Figure 5. Zeta potential of PP-SeNPs and SeNPs.

3.2. Acute toxicity of PP-SeNPs in mice

Acute toxicity testing showed a dose-dependent increase in mortality among mice administered PP-SeNPs (table 1). No deaths occurred at doses of 200-500 mg/kg, while mortality began to appear from 700 mg/kg and increased gradually at higher doses. Clinical signs in affected mice included reduced movement and decreased food intake within 1-2 h after administration. Based on the observed mortality distribution, the LD₅₀ of PP-SeNPs was calculated to be 945.83 mg/kg. Zhang et al. [25] prepared nano-Se using bovine serum albumin and reported an LD₅₀ value of 113 mg/kg, while chitosan-stabilized SeNPs showed an LD₅₀ of 258.2 mg/kg in the study by Zhai et al. [26]. Although LD₅₀ values of SeNPs vary widely depending on particle size, surface coating, and the specific LD₅₀ assessment procedure, the obtained LD₅₀ indicates that PP-SeNPs possess relatively low acute toxicity. This further suggests that PP serves as an effective biocompatible matrix that improves the safety profile typically associated with green-synthesized SeNPs.

Table 1. Acute toxicity test results of PP-SeNPs in white mice.

Group	Dose (mg/kg body weight)	Number of deaths within 72h	External manifestations during 0 – 72 h after oral administration
1	Control (distilled water)	0/6	Mice moved and ate normally, with normal light and sound reflexes.
2	200	0/6	Mice moved and ate normally, with normal light and sound reflexes.
3	500	0/6	Mice moved and ate normally, with normal light and sound reflexes.
4	700	1/6	Within 1–2 h, some mice showed reduced movement and reduced food intake.
5	850	2/6	Within 1–2 h, some mice showed reduced movement and reduced food intake.
6	1000	3/6	Within 1–2 h, some mice showed reduced movement and reduced food intake.
7	1100	5/6	Within 1–2 h, some mice showed reduced movement and reduced food intake.
8	1300	6/6	Within 1–2 h, some mice showed reduced movement and reduced food intake.

4. CONCLUSIONS

This study presents the first report on the green synthesis of selenium nanoparticles using PP as a capping and stabilizing agent. Material characterization demonstrated that PP molecules functionalized the SeNPs surface through hydrogen bonding and electrostatic interactions of hydroxyl and carboxylate groups, thereby controlling nanoparticle growth and enhancing their physicochemical properties. PP-SeNPs exhibited smaller particle size and a narrower size distribution (65 - 100 nm vs. 75 - 160 nm for uncapped SeNPs), along with markedly enhanced colloidal stability (-22.9 mV vs. -8.7 mV). The acute toxicity assessment further revealed a low toxicity profile for PP-SeNPs with an LD₅₀ of 945.83 mg/kg.

These findings identify pumpkin polysaccharides as an effective and biocompatible matrix for engineering stable SeNPs with improved physicochemical and biological characteristics. Future work should focus on evaluating the biological activities and in vivo performance of PP-SeNPs to better define their therapeutic potential.

Acknowledgements: This research is funded by Vietnam Academy of Science and Technology (Grant number VAST03.08/23-24).

REFERENCES

- [1]. L. V. Papp, J. Lu, A. Holmgren, and K. K. Khanna, "From selenium to selenoproteins: synthesis, identity, and their role in human health," *Antioxidants & Redox Signaling*, Vol. 9, No. 7, pp. 775–806, (2007).
- [2]. R. Yang, Y. Liu, and Z. Zhou, "Selenium and selenoproteins, from structure, function to food resource and nutrition," *Food Science and Technology Research*, Vol. 23, No. 3, pp. 363–373, (2017).
- [3]. Shahidin, Y. Wang, Y. Wu, T. Chen, X. Wu, W. Yuan, Q. Zhu, X. Wang, and C. Zi, "Selenium and selenoproteins: mechanisms, health functions, and emerging applications," *Molecules*, Vol. 30, No. 3, p. 437, (2025).
- [4]. N. Bisht, P. Phalswal, and P. K. Khanna, "Selenium nanoparticles: a review on synthesis and biomedical applications," *Materials Advances*, Vol. 3, pp. 1415–1431, (2022).
- [5]. K. Pyrzynska and A. Sentkowska, "Selenium species in diabetes mellitus type 2," *Biological Trace Element Research*, Vol. 202, pp. 2993–3004, (2024).
- [6]. K. Bai, B. Hong, J. He, Z. Hong, and R. Tan, "Preparation and antioxidant properties of selenium nanoparticles-loaded chitosan microspheres," *International Journal of Nanomedicine*, Vol. 12, pp. 4527–4539, (2017).
- [7]. A. Ahzaruddin, A. Tarmizi, S. H. Adam, S. A. Nasihah, N. N. Ramli, N. A. Ahfizah, A. Hadi, M. A. Mutalib, S. Gee, S. Tang, and M. H. Mokhtar, "The ameliorative effects of selenium nanoparticles (SeNPs) on diabetic rat model: a narrative review," *Sains Malaysiana*, Vol. 52, pp. 2037–2053, (2023).
- [8]. B. Hosnedlova *et al.*, "Nano-selenium and its nanomedicine applications: a critical review," *International Journal of Nanomedicine*, Vol. 13, pp. 2107–2128, (2018).
- [9]. N. Zhou, H. Long, C. Wang, L. Yu, M. Zhao, and X. Liu, "Research progress on the biological activities of selenium polysaccharides," *Food & Function*, Vol. 11, No. 6, pp. 4834–4852, (2020).
- [10]. J. Li, B. Shen, S. Nie, Z. Duan, and K. Chen, "A combination of selenium and polysaccharides: Promising therapeutic potential," *Carbohydrate Polymers*, Vol. 206, pp. 163–173, (2019).
- [11]. W. Chen *et al.*, "Synthesis and antioxidant properties of chitosan and carboxymethyl chitosan-stabilized selenium nanoparticles," *Carbohydrate Polymers*, Vol. 132, pp. 574–581, (2015).
- [12]. W. Y. Qiu, Y. Y. Wang, M. Wang, and J. K. Yan, "Construction, stability, and enhanced antioxidant activity of pectin-decorated selenium nanoparticles," *Colloids and Surfaces B: Biointerfaces*, Vol. 170, pp. 692–700, (2018).
- [13]. J. Wang *et al.*, "Selenium polysaccharide from sweet corn cob mediated hypoglycemic effects in vitro and untargeted metabolomics study on type 2 diabetes," *International Journal of Biological Macromolecules*, Vol. 281 (Pt 2), p. 136388, (2024).
- [14]. Z. Yang *et al.*, "Study on the mechanisms by which pumpkin polysaccharides regulate abnormal glucose and lipid metabolism in diabetic mice under oxidative stress," *International Journal of Biological Macromolecules*, Vol. 270 (Pt 2), p. 132249, (2024).

- [15]. A. Lu *et al.*, "Preparation of the controlled acid hydrolysates from pumpkin polysaccharides and their antioxidant and antidiabetic evaluation," *International Journal of Biological Macromolecules*, Vol. 121, pp. 261–269, (2019).
- [16]. T. T. T. Thanh, T. T. M. Quach, Y. Yuguchi, N. T. Nguyen, Q. V. Ngo, N. V. Bui, S. Kawashima, and C. D. Ho, "Molecular structure and anti-diabetic activity of a polysaccharide extracted from pumpkin *Cucurbita pepo*," *Journal of Molecular Structure*, Vol. 1239, p. 130507, (2021).
- [17]. M. Yao *et al.*, "Selenium nanoparticles based on *Morinda officinalis* polysaccharides: Characterization, anti-cancer activities, and immune-enhancing activities evaluation *in vitro*," *Molecules*, Vol. 28, No. 6, p. 2426, (2023).
- [18]. R. S. Ramaswamy *et al.*, "Acute toxicity and the 28-day repeated dose study of a Siddha medicine *Nuna Kadugu* in rats," *BMC Complementary and Alternative Medicine*, Vol. 12, p. 190, (2012).
- [19]. W. Chen, H. Cheng, and W. Xia, "Construction of *Polygonatum sibiricum* polysaccharide functionalized selenium nanoparticles for the enhancement of stability and antioxidant activity," *Antioxidants*, Vol. 11, No. 2, p. 240, (2022).
- [20]. X. Li *et al.*, "Preparation, characterization, and bioactivities of polysaccharide-nano-selenium and selenized polysaccharides from *Acanthopanax senticosus*," *Molecules*, Vol. 29, No. 7, p. 1418, (2024).
- [21]. A. Serrafi, A. Wikiera, K. Cyprych, and M. Malik, "Spectroscopic and microscopic analysis of apple pectins," *Molecules*, Vol. 30, No. 7, p. 1633, (2025).
- [22]. M. Güzel and Ö. Akpınar, "Valorisation of fruit by-products: Production characterization of pectins from fruit peels," *Food and Bioproducts Processing*, Vol. 115, pp. 126–133, (2019).
- [23]. P. Wulandari *et al.*, "Coordination of carboxylate on metal nanoparticles characterized by Fourier transform infrared spectroscopy," *Chemistry Letters*, Vol. 37, No. 8, pp. 888–889, (2008).
- [24]. N. S. Shehata *et al.*, "Selenium nanoparticles coated bacterial polysaccharide with potent antimicrobial and anti-lung cancer activities," *Scientific Reports*, Vol. 13, p. 21871, (2023).
- [25]. J. S. Zhang, X. Y. Gao, L. D. Zhang, and Y. P. Bao, "Biological effects of a nano red elemental selenium," *BioFactors*, Vol. 15, No. 1, pp. 27–38, (2001).
- [26]. X. Zhai, C. Zhang, G. Zhao, S. Stoll, F. Ren, and X. Leng, "Antioxidant capacities of the selenium nanoparticles stabilized by chitosan," *Journal of Nanobiotechnology*, Vol. 15, No. 1, p. 4, (2017).

TÓM TẮT

Tổng hợp và xác định các đặc trưng của nano selen được ổn định bởi polysaccharide từ bí đỏ

Nghiên cứu này trình bày phương pháp tổng hợp xanh của nano selenium (SeNPs) từ Na_2SeO_3 sử dụng acid ascorbic làm chất khử khi có mặt polysaccharide được chiết xuất từ bí đỏ. Polysaccharide từ bí đỏ (PP) được sử dụng làm chất ổn định và phân tán cho SeNPs - một vai trò chưa được báo cáo trong các nghiên cứu trước đây. Vật liệu được đặc trưng bằng các kỹ thuật UV-Vis, XRD, FTIR, SEM, TEM, EDX và đo thế zeta. Phổ FTIR cho thấy PP che phủ bề mặt SeNPs thông qua liên kết hydro và tương tác tĩnh điện giữa các nhóm hydroxyl và carboxylate. Ảnh hiển vi điện tử cho thấy PP cải thiện rõ rệt hình thái hạt của PP-SeNPs, tạo ra các hạt gần như hình cầu, phân tán đồng đều, với kích thước chủ yếu trong khoảng 65 - 100 nm (so với 75 - 160 nm của SeNPs không được bao phủ). Hơn nữa, độ bền keo của PP-SeNPs cũng được cải thiện đáng kể, thể hiện qua giá trị thế zeta âm hơn nhiều (-22,9 mV so với -8,7 mV của SeNPs). Thử nghiệm độc tính cấp cho thấy PP-SeNPs có độc tính thấp, với giá trị LD_{50} đạt 945,83 mg/kg. Các kết thu được chỉ ra triển vọng hứa hẹn của polysaccharide từ bí đỏ trong việc tạo ra nano SeNPs ổn định cho các ứng dụng y sinh học tiềm năng của chúng.

Từ khoá: Nano selen; Bí đỏ; Polysaccharide; Độ ổn định; Độc tính cấp.